

Laser Chem. 1988, Vol. 8, pp. 385–408
© 1988 Harwood Academic Publishers GmbH
Photocopying permitted by license only
Reprints available directly from the Publisher
Printed in the United Kingdom

IR Photodecomposition of CH_3COCF_3

R. FANTONI, E. BORSELLA, S. PICCIRILLO,†
A. GIARDINI-GUIDONI‡ and R. TEGHIL‡

*ENEA, Dip. TIB, US Fisica Applicata, Centro Ricerche Energia Frascati, C.P.
65-00044 Frascati, Rome, Italy*

(Received January 25, 1988; in final form April 15, 1988)

IR multiple-photon decomposition of 1,1,1-trifluoroacetone has been achieved in bulk by irradiating molecules with 970.55 cm^{-1} laser radiation. In collisional regime the onset of laser induced breakdown has been observed. Primary fragmentation and subsequent ion and radical secondary reactions have been monitored detecting the spontaneous luminescence with a gateable Optical Multichannel Analyzer.

KEY WORDS: 1,1,1-trifluoroacetone, fluorescence and phosphorescence spectra 33.50 Dg, multiphoton processes 33.80 Wz, chemiluminescence and chemical laser kinetics 80.40 Tc, photodissociation and photoionization 83.50 Et.

INTRODUCTION

(a) IR photodecomposition processes in polyatomic molecules

It has been widely demonstrated that IR photodissociation of polyatomic molecules occurs after multiple-photon absorption along a vibrational ladder.¹ In general many IR photons (e.g. 20–60) have to pile up in order to reach the first dissociation threshold of the electronic ground state. In collisionless regime coherent absorption occurs through the first few vibro-rotational levels of the molecule, whereas

† ENEA student.

‡ Ist. Chimica, Università della Basilicata (PZ) Italy and also Dip. Chimica, Università di Roma "La Sapienza" (RM) Italy.

one-photon transitions take place in the dense region of states called quasi-continuum which is below the dissociation threshold. It has been also demonstrated² that at high photon fluxes, several dissociation thresholds can be reached and the decomposition proceeds along different channels. In collisional regime many dissociation thresholds can be overcome also through collision aided energy transfers between different absorbing molecules. In the latter case by increasing laser energy the undissociated molecule can even reach the first electronically excited states and also electronically excited products can be obtained.³ A further increase in the laser energy and the subsequent collisional energy redistributions can lead some of the molecules to highly excited Rydberg states which decay through autoionization processes. A resonant laser induced breakdown is originated in this case, whose onset depends on the IR multiple-photon absorption cross section of the initially excited molecule and on the efficiency of the energy transfer processes.⁴

CO₂-laser induced breakdown has been previously observed in several different gases,⁵ also in the case of mono and diatomic species with no IR active vibrational mode and of polyatomic molecules completely off-resonant in the 9–11 μm region. The non resonant process depends strongly on the ionization potential of the molecules and, at low pressures in the absence of external preionization, on their multiphoton ionization cross section. High pressures, usually larger than one atmosphere, are required to sustain the electron cascading process which is responsible for the breakdown. Collisions provoke a large fragmentation accompanied by the formation of positively and negatively charged particles. All the fragments, as well as the undissociated parent molecules can contain a large excitation energy in their degrees of freedom (electronic, vibrational, rotational and translational). Analogous fragmentation patterns can be expected in the resonant laser induced breakdown, which differs from the former process in the mechanism of production of the electrons necessary to initiate and sustain the discharge. In fact vibrationally hot molecules have considerably lower ionization potentials and, for high levels of vibrational excitation, collisions between them can easily furnish the energy needed to overcome the breakdown threshold.

In the resonant laser induced breakdown highly excited and ionized atomic and diatomic species are produced as in plasma discharges, but much lower power and lower total pressure are required. Further-

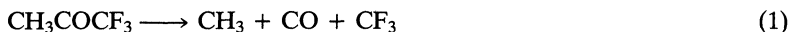
more, the laser process is not accompanied by an average increase of the temperature in the reactor, it allows to obtain spatial resolution and is not polluted by wall effects. Power threshold in the resonant laser induced breakdown is also in general lower than the one for the non resonant case; in fact, whatever mechanism is assumed for the production of the first electrons originating the cascading,⁵ vibrational excitation lowers the ionization potential of the molecules involved in the resonant laser induced process. These peculiarities make the resonant laser induced breakdown of potential interest for etching reactors. Fluorohydrocarbons, commonly used in plasma etching, are suitable species also for the laser assisted process. In fact these compounds have strong (C-F str.) and medium (C-C str.) IR absorption bands in the 9–11 μm region where the high power CO₂ laser is emitting.

The present study on CH₃COCF₃ molecule is carried on investigating the onset of all the different laser induced processes from the collisionless multiple-photon excitation to the resonant laser induced breakdown. By means of on line spectral and time resolved luminescence analysis, electronically excited transient species have been identified, their kinetics of formation and decay has been monitored as well. These diagnostics are especially suitable to supply the information necessary to design an etching experiment with different fluoroethanes and their larger homologues or derivatives.

(b) 1,1,1-trifluoroacetone molecule

CH₃COCF₃ has a vibrational mode overlapping with CO₂ laser emission around 970 cm^{-1} , which in analogy with CF₃COCF₃ molecule can be assigned to the antisymmetric C—C stretching.⁶

The dissociation energy for the C—C bond in CH₃COCH₃ is about 3.34 eV. In the case of hexafluoroacetone a value between 3.0 and 3.6 eV is estimated⁷ which corresponds to resonant absorption of 25–30 IR photons at $\approx 970 \text{ cm}^{-1}$ (0.12 eV each). Consequently, the lowest thresholds for 1,1,1-trifluoroacetone decomposition are expected to be around 3.3 eV and can be schematized as follows:



The energetics of 1,1,1-trifluoroacetone is expected to be quite similar to the acetone and hexafluoroacetone case, when CH_3COCF_3 molecules are resonantly excited with the 10R12 CO_2 laser line. Analogously with previous results on hexafluoroacetone⁷ and pentafluoroacetone⁸ IR laser induced decomposition, the dissociation is expected to occur through CO elimination and secondary radical reactions following after (1). Decomposition leading to acetyl as primary product (reaction (2)) should be hardly detectable since both CH_3CO and $(\text{CH}_3\text{CO})_2$ are still resonant with the 10 μm CO_2 laser radiation.⁹ Furthermore, the well-known instability of the trifluoroacetyl radical at room temperature⁷ rules out a decomposition leading to formation of fluorinated biacetyls through this intermediate (reaction (3)). However, the formation of biacetyl has been observed in direct u.v. photodissociation of acetone and 1,1,1-trifluoroacetone.^{10,11} In the case of IR laser induced decomposition of hexafluoroacetone, final products after reaction (1) were hexafluoroethane and carbon monoxide, minor amounts of CF_4 and C_2F_4 were also detected at high conversion.⁷ Similar products are expected to be formed in the analogous experiment on 1,1,1-trifluoroacetone.

EXPERIMENTAL

1,1,1-trifluoroacetone molecules were excited by using multimode, line-tunable pulsed T.E.A. CO_2 laser (a Lumonics module 102 and a home-made two module oscillator + amplifier). Both the sources were operated with a 65:30:11 He: CO_2 : N_2 atmospheric gas mixture. The typical pulse shape consisted of a 100 ns (FWHM) peak followed by a tail of about 1.5 μs , as observed by monitoring on a 400 MHz oscilloscope (TEK 7844 dual beam oscilloscope) the signal coming from a fast detector (Molelectron mod. P3-00, with ns rise-time).

The laser radiation was either gently or tightly focussed in the center of each reaction cell by using NaCl and ZnSe lenses with different focal lengths. Laser power was evaluated by measuring at the entrance of the reaction cell the laser energy on a pyroelectric detector (Gen-Tec model PRJ-D) and the beam cross section at the focus inside the empty cell (as burnt patterns on thermosensitive paper).

IR laser induced decomposition of 1,1,1-trifluoroacetone has been investigated in different reaction cells either by final product analysis

or by monitoring on-line, with spectral and time analysis, the chemiluminescence emitted by electronically excited molecules and radicals formed after absorption of the laser radiation. The cubic reactor ($l = 180 \text{ nm}$) used for chemiluminescence analysis has been equipped with two parallel metallic plates (with a separation of 22 mm) placed along the focal region of the CO_2 laser. By setting a small potential difference (e.g. $\pm 50 \text{ V}$) across the plates, it is possible to detect electronic or ionic current pulses if the chemiluminescence is induced by electron impact in a breakdown discharge. Ion and electron currents were recorded on a 40 MHz bandwidth digital oscilloscope (TEK 2430).

(a) Final product analysis

IR photodecomposition of 1,1,1-trifluoroacetone has been achieved in a small cell ($l = 20 \text{ mm}$, $d = \text{mm}$). Single shot product analysis was directly performed connecting the cell to a gas chromatograph equipped with a Porapak column and a flame ionization detector. A gently focussed irradiation geometry was chosen (laser energies between 0.1–0.7 J; laser fluences between 0.5–1.5 J/cm^2).

(b) Analysis of the chemiluminescence

The stainless steel vacuum chamber was pumped by a 450 l/sec turbomolecular pump and the background pressure was less or equal to 10^{-5} Torr.

The visible luminescence emitted from the fragments was observed perpendicularly to the laser beam through a quartz window. A quartz lens ($f = 250 \text{ mm}$) focussed the emitted light on the entrance slit of a 320 mm focal spectrograph supplied with a 150 grooves/mm grating. An EG & G Optical Multichannel Analyzer (OMA III) was employed for simultaneous detection of the luminescence spectrum. An intensified photodiode array detector (512 elements) was mounted at the exit of the spectrograph and the luminescence spectrum was acquired with a resolution of approximately 0.5 nm per channel—as measured on the resolved 579.07 nm – 576.96 nm Hg doublet. The sensitivity (photon/counts) of the detector (EG & G 1420 BR-512-G) at three points across the spectral range (180–900 nm) is: 8 at 300 nm,

15 at 550 nm and 67 at 830 nm. The detector was either operated with a fixed exposure time of 16 ms or gated by a high voltage pulse generator (EG & G model 1211) with fast rise and fall times; a time resolution better than 40 ns was achieved in the latter configuration. When the luminescence signal was too weak to be detected by the O.M.A. system, the time behaviour of the full spectrum was monitored through a EMI 9658B (S20/B Spectral Response) photomultiplier. The photomultiplier output was fed to a digital oscilloscope (TEK 2430) with 40 MHz bandwidth.

More details on the experimental apparatus used for the analysis of the chemiluminescence can be found in reference (12), where the same apparatus has been employed to investigate SiH₄ laser induced decomposition.

RESULTS AND DISCUSSION

(a) Dissociation without emission

High purity 1,1,1-trifluoroacetone was purchased from PCR in a stainless steel cylinder and used without further purification. In the pressure range 1 Torr $\leq p \leq$ 20 Torr the sample was irradiated at 970.55 cm⁻¹ either pure or with addition of other species (i.e. noble gasses and acetone). When pure CH₃COCF₃ was irradiated at low laser fluence ($\phi < 1.5$ J/cm²) and low pressure ($p \leq 10$ Torr) no chemiluminescence from products formed in electronically excited states was observed either by bare eye or by a photomultiplier. However an increase in the total pressure indicated the occurrence of dissociation; reaction (1) is indeed accompanied by a pressure increase. Only one threshold for 1,1,1-trifluoroacetone decomposition was found at ≈ 1.0 J/cm² (value at 1 Torr) corresponding to the formation of one product detected by the gas chromatograph. This product has been identified as 1, 1,1-trifluoroethane which corresponds to the opening of channel (1) and the overall CO elimination reaction. The same dissociation pattern has been observed by Hackett and Willis⁷ in IR photodecomposition of hexafluoroacetone. It is also known that thermal decomposition of 1,1,1-trifluoroacetone leads to CO elimination.¹³ Pyrolysis of hexafluoroacetone around 600°C demonstrated¹⁴ the occurrence of CO elimination and the opening of a

second channel which leads to $\text{CF}_3\text{COF} + \text{CF}_2$ at higher temperatures. We observed that the threshold for IR decomposition of 1,1,1-trifluoroacetone is lower by increasing the total pressure, especially when an efficient collisional partner, such as Ar or Kr, is added.

(b) Dissociation accompanied by visible—u.v. emission

By increasing either the laser power or the total pressure different luminescence emissions were observed by bare eye. A white emission was easily obtained gently focussing the laser beam in the cell. A very intense white emission with delayed blue-green components was seen by tightly focussing the laser beam in the centre of the reaction cell.

At 10 Torr of pure CH_3COCF_3 for laser fluences larger than 1.5 J/cm^2 and smaller than 8 J/cm^2 a characteristic broad u.v.-visible emission is observed. The emission spectrum detected by an Optical Multichannel Analyzer (exposure time 16 msec) is shown in Figure 1(a), its decay in time was measured by using a photomultiplier and is reported in figure 1(b). The CH_3COCF_3 u.v. absorption band is centered at 285 nm, and broad red shifted fluorescence and phosphorescence bands, extending from 330 nm to 550 and from 400 nm to 600 nm respectively, have been found in (15). The spectrum here reported (Figure 1(a)) shows an intense broad band extending from 380 nm to the near IR which, assuming an average level of excitation between 3.0 and 4.0 eV, can be the envelope of the fluorescence and phosphorescence emissions observed in (15); a resonance fluorescence channel, exactly corresponding to the u.v. absorption band, should be responsible of the other emission band observed between 280 nm and 380 nm. The time profile of the whole spectrum—measured with the photomultiplier—can be separated in a fast (from the fit $\tau_1 = 1.5 \mu\text{sec}$ at 10 Torr) and slow component (from the fit $\tau_2 = 94 \mu\text{sec}$ at 10 Torr). The fast component probably accounts for fluorescence and the slow one for phosphorescence channels; the fast component of the time decay is affected by the laser pulse time duration ($\approx 1.5 \mu\text{sec}$), in fact fluorescence lifetimes of only a few nsec have been obtained in reference (15, 16). The scheme of electronic levels of 1,1,1-trifluoroacetone results to be very similar to the one proposed by Costela *et al.*¹⁷ for acetone. In fact, both the spectral emission and the time decay are consistent with de-excitation of the first 1,1,1-trifluoroacetone electronic states ($S_1(A)$) at 3.66 eV coupled with the

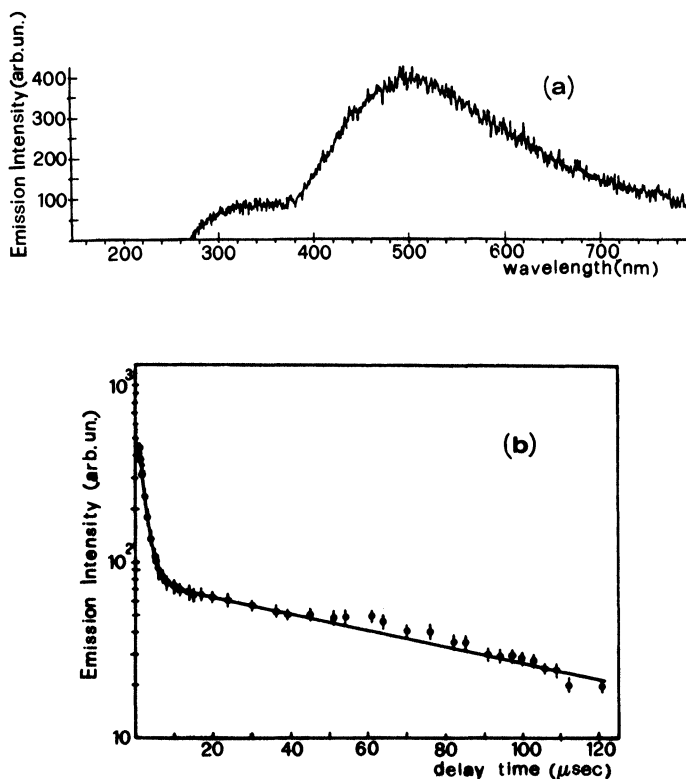


Figure 1 Luminescence signal emitted from 10 Torr of CH_3COCF_3 irradiated with 1.5 J/cm^2 at 970.55 cm^{-1} : (a) overall emission spectrum detected by the O.M.A. system (16 msec exposure time, 20 laser shots); (b) time profile of the whole spectrum measured by the photomultiplier.

first electronically excited dissociative channel T_1 at 3.25 eV^{15}). However, in the green-red tail of the spectrum here measured emission from the acetyl radicals and the biacetyl molecules formed in electronic excited states (at 2.72 eV and 2.47 eV) could be also present to account for the intensity measured for $\lambda \geq 460 \text{ nm}$. In fact the existence of fluorescence ($A^1A_g \rightarrow X^1A_g$ in the range 460 nm – 600 nm) and phosphorescence ($a^3B_g \rightarrow X^1A_g$ in the range 501.4 nm – 613.5 nm) bands for the excited biacetyl molecule is well-known.^{9–11,18}

In these experimental conditions it has been verified that we are far from the onset of a resonant IR laser induced breakdown, since no ion and electron current was collected on two electrodes placed close to the centre of the reaction cell. This is not unexpected for an average level of excitation lower than 4.0 eV, as assumed in the former discussion, which is far from the 1st molecular ionization potential—at 9.70 eV for acetone.¹⁸

(c) Dissociation with emission from excited CO

When laser fluence is over 2.5 J/cm² and some Ar is added (e.g. 10 Torr, 1,1,1-trifluoroacetone + 20 Torr Argon) a much higher average level of excitation can be reached by undissociated molecules. In fact, under these conditions up to 5–6 J/cm², highly excited molecular states (e.g. the S₁(D)—at 8.07 eV for acetone¹⁸—and its neighbouring triplet states) just below the Rydberg series can be populated. These states, which correspond to electronic excitation strongly localized on the CO group in the molecule, will lead to molecular dissociation which produces CO in the corresponding electronically excited states (A¹Π, e³Σ⁻, d³Δ_i, a^{'3}Σ⁺ and a³Π_r at 8.07 eV, 7.96 eV, 7.58 eV, 6.92 eV and 6.04 eV, respectively¹⁹). Peculiar CO* line emission is observed in Figure 2(a) overlaid to the broad molecular spectrum (cfr. Figure 1(a)). Especially meaningful is the 190–290 nm u.v. emission reported in Figure 2(b). According to references (19, 20) in this region CO emissions known as the 4th positive system (from A¹Π to the ground state X¹Σ⁺) and the Cameron band (from the a³Π_r to the ground state) are expected. By using the emission line-positions and intensities given in reference (20) without any information on CO average temperature, we have tried to simulate the spectrum in this region assuming a convolution of gaussian peaks with 1.5 nm F.W.H.M. accounting for experimental resolution, and power and pressure broadenings. As Figure 2(c) shows main features of the experimental spectrum are reproduced, and then can be ascribed to the mentioned CO transitions. These emissions, which largely dominate the spectrum since they also appear at the second and third order of the grating, are only occurring in the first few μsec after the laser excitation. Later line emission from CO is also observed in the visible which is mainly due to transitions between triplet excited states: the triplet band (from the d³Σ⁻ to the a³Π_r) and the Asundi band (from the a^{'3}Σ⁺ to the a³Π_r^{19,20}).

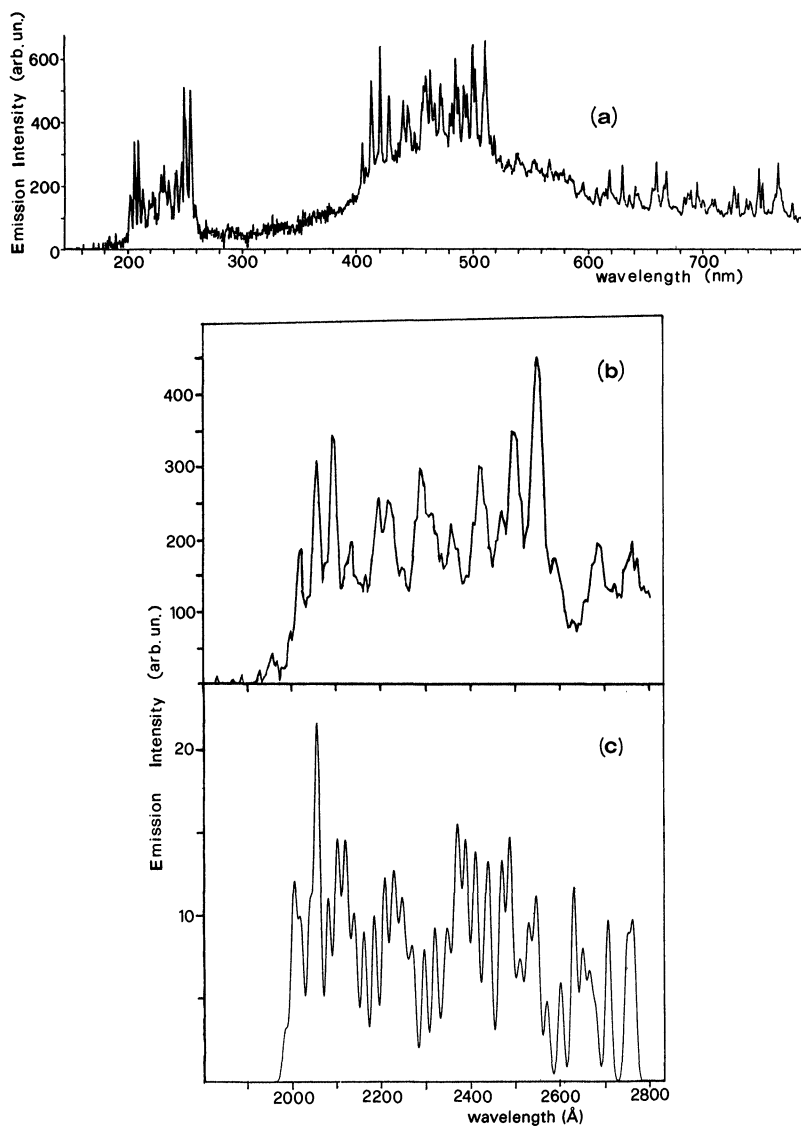


Figure 2 Chemiluminescence spectrum emitted from 10 Torr of CH_3COCF_3 + 20 Torr Ar irradiated with 2.5 J/cm^2 at 970.55 cm^{-1} ; (a) overall emission spectrum detected by the O.M.A. system (16 msec exposure time, 100 laser shots); (b) section of the time-resolved single-shot spectrum measured $0.8 \mu\text{sec}$ after the laser pulse, gate width $1.0 \mu\text{sec}$; (c) reconstructed CO emission in the range 180–280 nm from data of reference (20).

Also in these experimental conditions no ions or electrons have been detected. A schematic of CO energy levels from¹⁹ is drawn in Figure 3, where some electronically excited levels of CH₃COCH₃ from (18) are also reported for comparison since there are not enough literature data for a direct comparison with CH₃COCF₃; in this figure the right scale corresponds to the average number of I.R. photons at 970 cm⁻¹ which should be supplied to the molecule to reach a given electronic state. From the data shown in Figure 2 and the diagram in Figure 3 we conclude that in collisional regime the 1,1,1-trifluoroacetone molecule can store more than 66 IR photons and primarily decomposes according to channel (1), giving rise also to CO in the A¹Π state. Note that the a³Π state is probably coming from a lower threshold channel close to the S₁(B) state—at 6.35 eV for acetone—reached with 54 photons. Successive CO triplet emission is probably induced by collisions which populate the d³Σ⁻ and the a³Σ⁺ levels.

(d) Laser induced breakdown

Within this picture a further increase in the laser fluence will cause occurrence of the laser induced resonant breakdown. Indeed long lasting ion and electron currents (peak FWHM ≈ 60 μsec, Figure 4), whose intensity and time profile depends on the presence of different noble gases, are detected on the electrodes as soon as molecular excitation proceeds through Rydberg states. The first molecular ionization potential (I.P. = 9.70 eV for CH₃COCH₃) is overcome at laser fluence 10 J/cm² ≤ φ ≤ 20 J/cm² conditions and superexcited molecular states can be produced. Radiative decay or preionization can take place from the parent molecule and from the radical fragments.²¹ It has been verified that addition of different noble gases alters these current peaks noticeably, probably because collisions lead to formation of highly excited long living metastable or autoionizing states of the noble gas. For instance, in the case of addition of Ar to CH₃COCF₃, two metastable levels of Ar (3p⁵4s ³P₂ and 3p⁵4s ³P₀), whose lifetimes are of the order of seconds²² can act as energy reservoirs at 11.55 eV and 11.72 eV respectively, after being formed in the initial discharge.

In the laser induced breakdown a bright luminescence is observed by bare eye; the colour of the discharge is initially white and promptly turns to blue-green. The full emission spectra recorded in the 160–

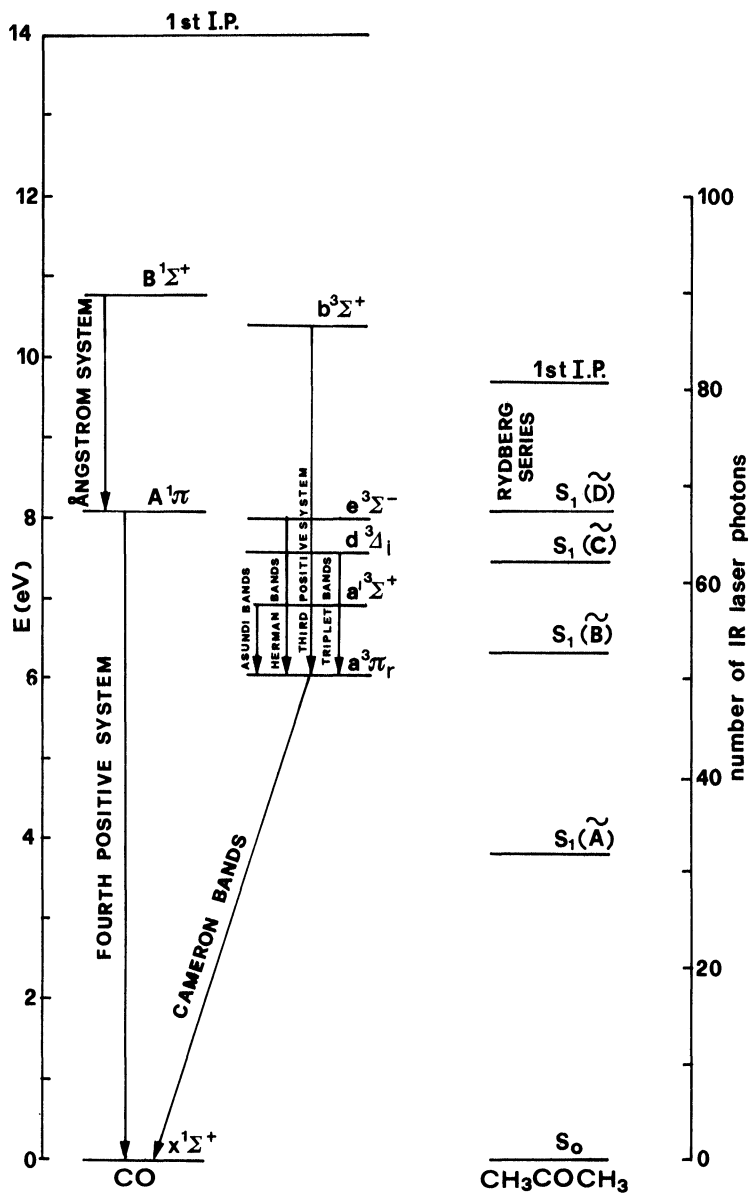


Figure 3 Schematic of CO¹⁹ and CH₃COCH₃¹⁸ electronically excited energy levels. Some CO emission bands are indicated as well.

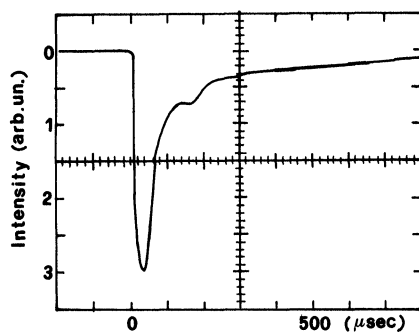


Figure 4 Electron currents measured on the electrodes (50 V applied) in the resonant laser induced breakdown of CH_3COCF_3 (10 Torr) at 970.55 cm^{-1} with 20 J/cm^2 . The ion peak had the same profile but opposite sign.

760 nm range, with an exposure time of 16 msec is shown in Figure 5 where arrows mark the assignment of main features. This spectrum is peculiar of hydrocarbon and fluorohydrocarbon discharges, in fact we have detected with the same experimental set-up very similar spectra in the laser induced breakdown of C_2H_4 and C_3H_6 (both irradiated at 947.74 cm^{-1}), apart from fluorinated species and CO emission. No overall change in the spectral emission is observed when different atoms (He, Ar, Kr) or molecules (CH_3COCH_3) are added. The time evolution of the emission spectrum is shown in Figure 6(a)–6(d) for a 1:1 mixture of 1,1,1-trifluoroacetone in Ar (20 Torr total pressure). In

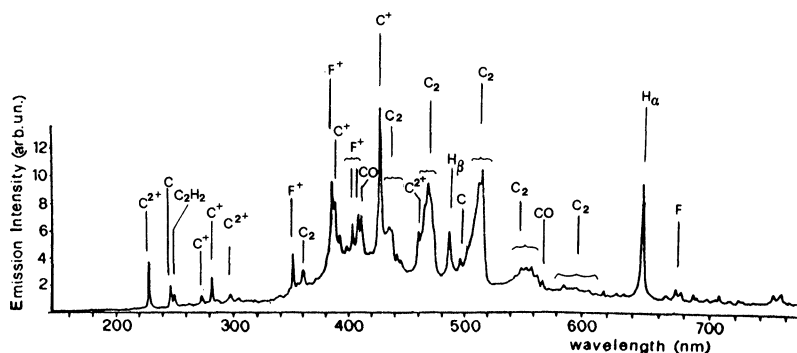


Figure 5 Chemiluminescence spectrum measured in the resonant laser induced breakdown of CH_3COCF_3 (10 Torr) with 20 J/cm^2 laser fluence at 970.55 cm^{-1} , 10 laser shots, 16 msec exposure time.

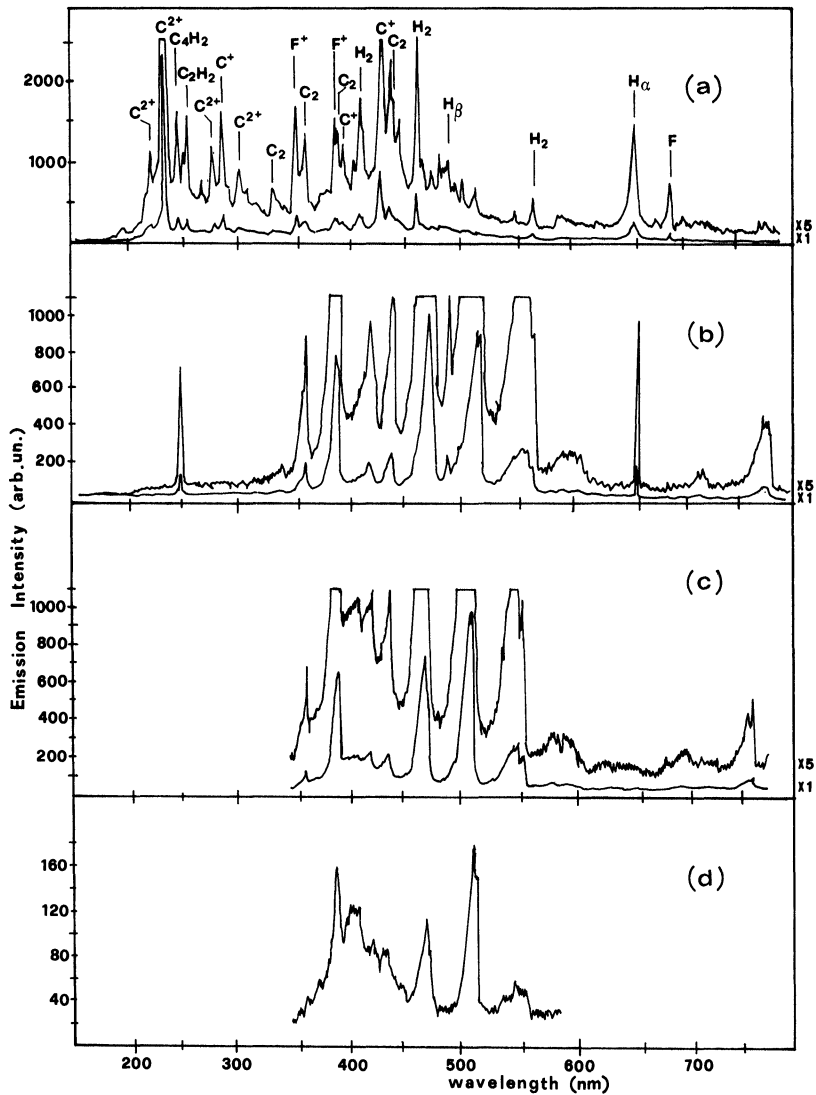


Figure 6 Chemiluminescence spectra measured in the resonant laser induced breakdown of CH_3COCF_3 with 20 J/cm^2 laser fluence at 970.55 cm^{-1} , single shot emission spectra of 10 Torr sample + 10 Torr Ar: (a) measured $1.0 \mu\text{sec}$ after the laser pulse, gate width $1.0 \mu\text{sec}$; (b) measured $10.0 \mu\text{sec}$ after the laser pulse, gate width $1.0 \mu\text{sec}$; (c) measured $50.0 \mu\text{sec}$ after the laser pulse, gate width $10.0 \mu\text{sec}$; (d) measured $120.0 \mu\text{sec}$ after the laser pulse, gate width $20.0 \mu\text{sec}$.

these measurements a gate on the O.M.A. system has been set with variable delay and exposure times. Identification of the observed peaks is reported in Table I; arrows mark the assignment of main features in Figure 6(a) as well. Most of the u.v. emission is ascribable to singly and doubly charged Carbon ions and accounts for the initial white light. Ionic states with an appearance potential around 40 eV are reached during the laser pulse (e.g. $6g^3G_{3-5}$, $df^1F_3^o$ and $3s^1P_1^o$ at 44.47 eV and 38.44 eV, respectively²³). The time decay of most of these

Table I Identification of ionic (a), atomic (b), and molecular (c) fragments in the laser induced breakdown of CH₃COCF₃; corresponding spectra are reported in Figure 5 and Figure 6.

<i>(a) Ionic fragments (assignment according to (23))</i>	
species	emission wavelength (nm)
C ⁺²	216.3 229.7 272.5 272.5 272.6 298.2
C ⁺	283.7 283.8 391.9 392.1 426.7 426.7 513.3
	513.3
CH ⁺ (from C ⁺ 4P)	316.3 334.8 342.1 356.2 363.5
F ⁺	350.1 350.3 350.6 384.7 385.0 385.2 402.5
	402.5 402.6
<i>(b) Atomic fragments (assignment according to (23))</i>	
species	emission wavelength (nm)
C	193.1 247.9
H	486.1 (H _β) 656.3 (H _α)
F	624.0 677.4 683.4 685.6 687.0 690.3 720.2
	731.1 775.5
<i>(c) Molecular fragments (assignment according to (20))</i>	
sp-ecies band	emission wavelength (nm)
C ₄ H ₂ $\bar{A} \leftarrow X$	239.5 243.3 265.0 265.1
C ₂ H ₂ $\bar{A} \leftarrow X$	246.6 249.9
C ₂ Deslandres-D'Azambuja	358.8 385.2 410.2
C ₂ High pressure	435.3 436.9 466.3 468.0 587.8 590.0 642.0
	644.2
C ₂ Swan	436.5 437.1 438.3 466.9 467.9 468.5 469.8
	471.5 473.7 509.8 512.9 516.5 547.1 550.2
	554.1 558.6 563.6 592.3 595.9 600.5 606.0
	612.2 619.1
CO Triplet	401.1 418.8
H ₂ Singlet and triplet	406.7 407.0 417.1 456.3 457.6 458.0 458.3
	461.8 462.8 463.2 527.2 529.2 530.3 555.2
	559.8 561.3 565.6 577.5 582.3 587.9 588.8
	593.1 595.0 597.5 599.4 600.3 602.8 603.2
	608.1 616.2 618.3
F ₂ Gale-Monk	610.3 651.9

states is very fast (typically in a discharge with 10 Torr of pure 1,1,1-trifluoroacetone a value of $0.62 \mu\text{sec}$ is obtained for the intense peak at 230 nm attributed to C^{+2} emission from the $^1\text{D}_2 \text{C}^{+2}$ level at 18.09 eV). A low lying quartet state of $\text{C}^+(^4\text{P})$ at 5.33 eV is also populated, this states is not observed in emission but its presence is inferred from the formation of CH^+ in an excited state after a secondary reaction with H_2 ($\text{b}^3\Sigma^+ \rightarrow \text{a}^3\Pi \text{CH}^+$ emission).²⁴ Only a few ions show also delayed emission a long time (10 μsec) after the laser pulse. Atomic (C, F, H)²³ and molecular (C_2 , H_2 , CO)^{19,20} emission especially from Rydberg states dominate the delayed spectra; these lines are coming from energy levels between 4 eV and 20 eV.

At very long delay times (over 100 μsec) emission is only due to the parent molecule and the C_2 fragment; all the states involved are lower than 5 eV in energy. In particular the C_2 excited states $\text{C}^1\Pi_g$ at 4.25 eV and $\text{d}^3\Pi_g$ at 2.48 eV, which give rise respectively to Deslandres-D'Azambuya's and Swan systems (including the high pressure bands²⁰ in the latter) are very close 1,1,1-trifluoroacetone triplet states which in turn are assumed to be coupled to dissociative channels.¹⁵⁻¹⁷ The time decay of the broad band emission (in the range 380–440 nm) is assigned to the parent molecule and has been fitted with a double exponential decay ($\tau_1 = 18 \mu\text{sec}$ and $\tau_2 = 84 \mu\text{sec}$ —Figure 7(a)) which fits as well the decay of the peaks belonging to the Swan system (Figure 7(b)). Faster decay constants have been found for the Deslandres-D'Azambuya's peaks ($\tau_1 = 12 \mu\text{sec}$ and $\tau_2 = 39 \mu\text{sec}$ —Figure 7(c)), this fact can be due to a more efficient collisional deactivation of the upper excited state. In our opinion the two decays correspond with phosphorescence from the first two molecular triplet states which are both coupled to dissociative channels, the second one having a smaller barrier for dissociation (as in the case of acetone).¹⁷ A large fragmentation seems to occur as soon as CH_3COCF_3 has overcome the barriers for dissociation in these triplet states. Present data seem to support the hypothesis that the electronically excited C_2 is the main product of collisionally induced dissociation, in which it retains some of the electronic excitation and thus it is seen in emission. The rise-time of C_2 emission in the Swan system ($\approx 3 \mu\text{sec}$, see data in Figure 8) should account for the C_2 production in the molecular dissociation process, whereas the long time-decays are related to the slower fragmentation processes; in fact the $\text{C}^1\Pi_g$ and the $\text{d}^3\Pi_g$ radiative life-times are rather short, 5 nsec and 185 nsec, respectively.²⁰

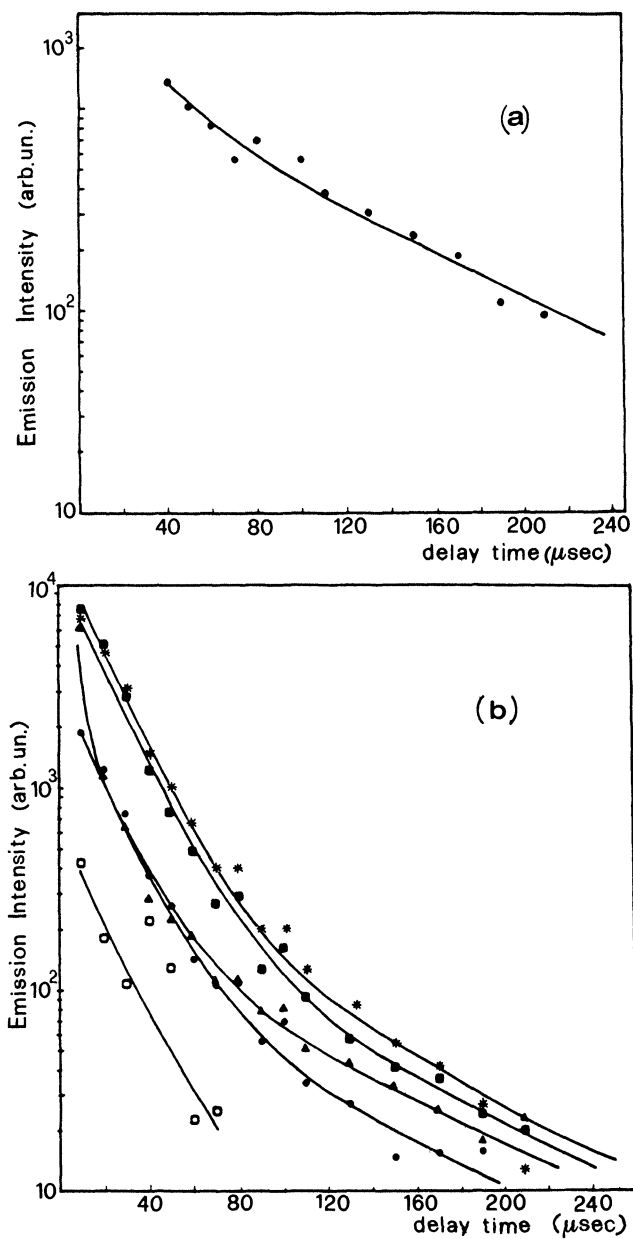


Figure 7 (a,b) Time profile of different molecular peaks from the time resolved spectra measured with the O.M.A. system on 10 Torr CH_3COCF_3 + 10 Torr Ar with 20 J/cm^2 at 970.55 cm^{-1} : (a) CH_3COCF_3 emission at 400 nm; (b) C_2 emission in the Swan system \blacktriangle at 437 nm, $*$ at 471 nm, \blacksquare at 516 nm, \bullet at 558 nm, \square at 606 nm. Full curves are the best fit of the data with $\tau_1 = 18 \text{ } \mu\text{sec}$ and $\tau_2 = 84 \text{ } \mu\text{sec}$.

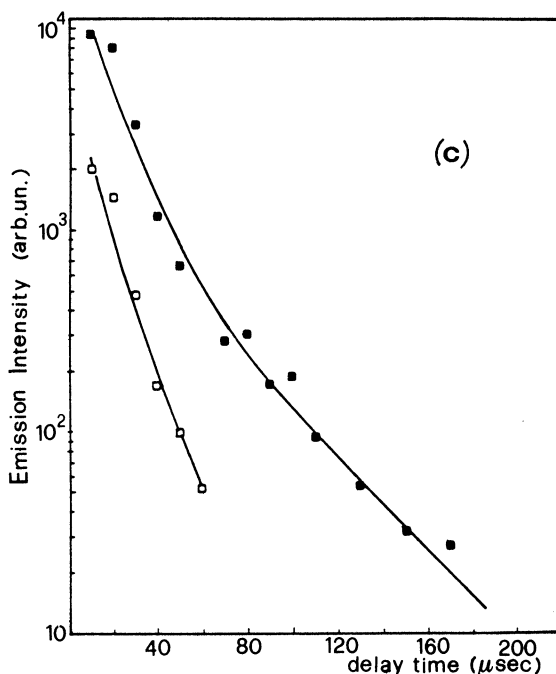


Figure 7(c) Time profile of different molecular peaks from the time resolved spectra measured with the O.M.A. system on 10 Torr CH_3COCF_3 + 10 Torr Ar with 20 J/cm^2 at 970.55 cm^{-1} ; (c) emission in the Deslandres-D'Azambuja's system □ at 359 nm, ■ at 385 nm. Full curves are the best fit of the data with $\tau_1 = 12 \text{ } \mu\text{sec}$ and $\tau_2 = 39 \text{ } \mu\text{sec}$.

The production of C_2 molecules is a general phenomenon in discharges in hydrocarbons. In fact C_2 absorption (detected by LIF) and emission in the Swan band has been also observed in all cases of hydrocarbon IR multiple-photon excitation at high laser power even in experiments carried out at very low pressure (a few mTorr).²⁵ To this respect we should mention that the growth of solid Carbon particles could also be responsible for the late C_2 production followed by the long lasting emission (Figure 7(a)–(b), Figure 8). In fact at high decomposition rates a solid dark deposit was formed on the surfaces (hot spots) of the optical windows. The investigation of the early time evolution (1 μsec –10 μsec delay from the laser pulse) of excited C_2 emission intensity—reported in Figure 8—seems to suggest a possible relation between solid particle nucleation and the delayed C_2 emission. The data, taken both on 10 Torr of pure sample and in a 1:1 mixture in

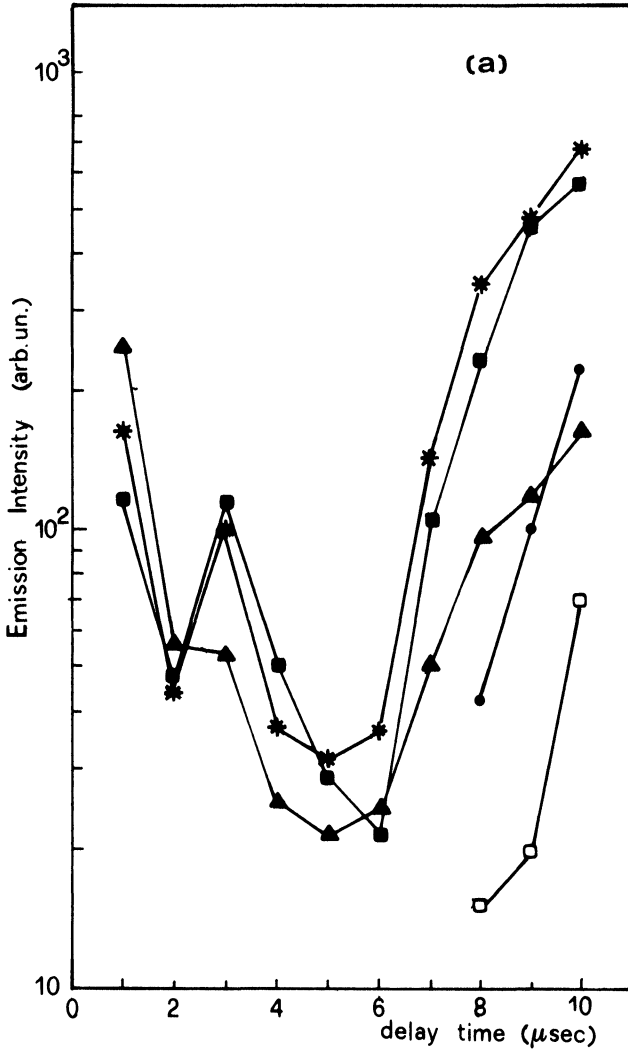


Figure 8(a) Time profile of different C_2 peaks in the Swan system from the time resolved spectra measured with the O.M.A. system on 10 Torr CH_3COCF_3 , laser fluence 20 J/cm^2 at 970.55 cm^{-1} . Emission ▲ at 437 nm, * at 471 nm, ■ at 516 nm, ● at 558 nm, □ at 606 nm. The lines on the experimental data are smooth curves drawn through the data to aid visualization.

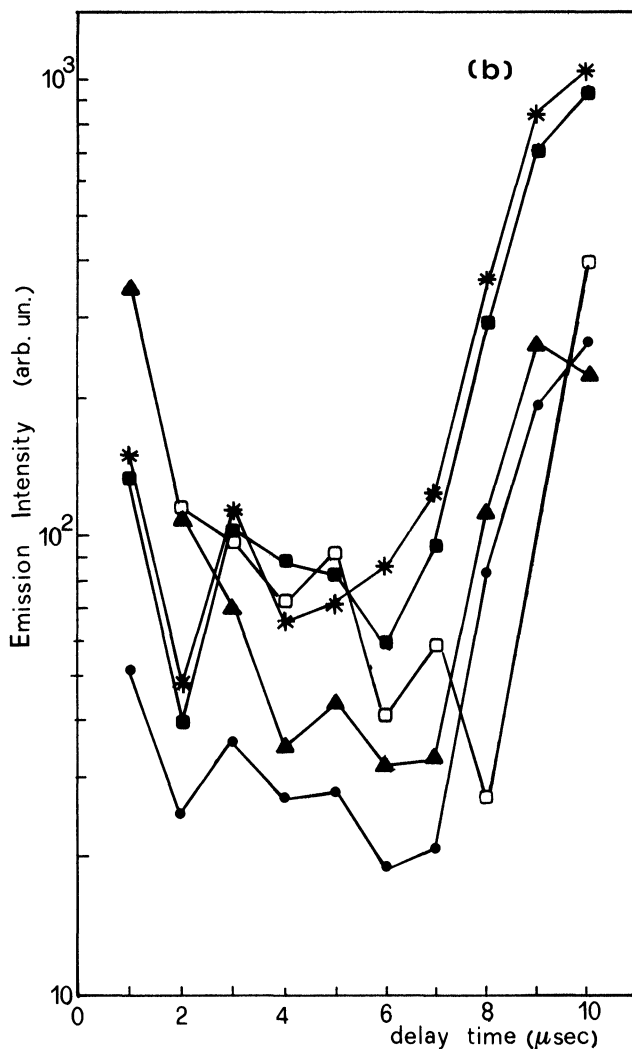


Figure 8(b) Time profile of different C₂ peaks in the Swan system from the time resolved spectra measured with the O.M.A. system on 10 Torr CH₃COCF₃ + 10 Torr Ar, laser fluence 20 J/cm² at 970.55 cm⁻¹. Emission ▲ at 437 nm, * at 471 nm, ■ at 516 nm, ● at 558 nm, □ at 606 nm. The lines on the experimental data are smooth curves drawn through the data to aid visualization.

Argon, show that the $\text{C}^1\Pi_g$ and the $\text{d}^3\Pi_g$ states are promptly formed and initially decay with time constants of the order of 1–2 μsec . The large increase in the whole C_2 emission observed after $\approx 6 \mu\text{sec}$ (with a relative maximum between 9 μsec delay) could be related with the growth of solid carbon grains still retaining some excitation in a C_2 group. An analogous hypothesis can be made in case of Si and Si_2 emission observed—directly by L.I.F.—in SiH_4 chemical vapour deposition which has been related to solid silicon nucleation and growth.²⁶

(3) Pressure effect in resonant laser induced breakdown

Pressure effects in the resonant laser induced breakdown of 1,1,1-trifluoroacetone have been investigated at 20 J/cm^2 laser fluence. We have observed that the pressure threshold for laser induced breakdown is ≈ 10 Torr and that the increase of the concentration of the resonant molecule up to 50 Torr is detrimental to the chemiluminescence yield of the species produced in the spark. However the increase in the total pressure favours the process by lowering the pressure threshold—down to less than 5 Torr—by addition of other species (i.e. noble gasses, non resonant molecules) up to ≈ 100 Torr. These findings can be explained taking into account both the mechanism of the process and the geometry of irradiation. Dealing with a collisional dissociation mechanism, the increase of the total pressure is expected to favour the process. On the other hand the increase in concentration of the resonant species in the cell gives rise to a strong absorption which makes the laser power available in the focus insufficient to provoke the breakdown phenomenon.

CONCLUSIONS

The occurrence of resonant laser induced breakdown in 1,1,1-trifluoroacetone has been demonstrated at moderate laser powers ($\approx 3\text{MW}/\text{cm}^2$ for 10 Torr CH_3COCF_3 in Ar or Kr at 30 Torr total pressure), by using a T.E.A. CO_2 pulsed source to excite a medium-weak IR band ($\mu \approx 0.08 \text{ D}$).

Large fragmentation of the parent molecule has been observed with early formation of hot ionic species. Atomic fluorine, hydrogen and carbon are produced in the microsecond scale. Late dissociation of the

CH_3COCF_3 molecule gives probably rise to the longer lasting production of C_2 which has been detected in several electronically excited states. Work is in progress in order to ascertain if this late C_2 could be related to the growth of solid Carbon particles. In fact, if this is the case and if it is a general phenomenon for both hydrocarbon and hydrosilicon compounds, an important parameter relevant to laser induced chemical vapour deposition (the growth) can be directly obtained through the employed emission spectroscopy.

In conclusion the fragmentation following the resonant laser induced breakdown is quite different from collisionless and collisional multiple-photon dissociation. The breakdown process allows to obtain on a short time scale high concentrations of atomic species interesting for etching. Furthermore the production of small hydrocarbon fragments (e.g. C_2 and CO) on a longer time scale could be advantageous in surface photopolymerization.

Resonant laser induced breakdown, as well as the non-resonant process occurring at higher laser power, is also suitable to be used for chemical analysis detecting spark emission spectra²⁷ similar to the ones reported in this paper. L.I.F. has been already successfully employed to monitor the concentration of the etchant molecule and of the fragments in a plasma etching reactor.²⁸ As shown in this paper, in a resonant laser induced breakdown the analysis of the emission spectra can supply an analogous piece of information by monitoring the formation and decay of different excited species.

Acknowledgements

D. Consalvo and Dr. L. Caneve are gratefully acknowledged for participating in some of the measurements taken at ENEA Frascati.

Thanks are due to Professor A. Mele for suggesting the study of CH_3COCF_3 and supporting the work on the final product analysis performed in the Chemistry Department of the University of Rome.

The work of Dr. S. Loreti and M. Snels in building the T.E.A. CO_2 laser amplifier at the University of Rome is also gratefully acknowledged.

References

1. C. D. Cantrell, V. S. Letokhov and A. A. Makarov in "Coherent nonlinear optics," Eds. M. S. Feld and V. S. Letokhov (Springer-Verlag, Berlin, 1980), pp. 165-269; A. Giardini-Guidoni, E. Borsella and R. Fantoni, *Ber. Bunsenges. Phys. Chem.* **89**, 286 (1985); D. W. Lupo and M. Quack, *Chem. Rev.* **87**, 181 (1987).
2. A. M. Ronn in "Photoselective chemistry," J. Jortner, R. D. Levine and S. A. Rice Eds. (Interscience Publication, New York, 1981), pp. 661-677; H. Reisler, C. Wittigin

- "Photoselective Chemistry," J. Jortner, R. D. Levine and S. A. Rice Eds. (Interscience Publication, New York, 1981). pp. 679-711; Y. Haas in "Photoselective Chemistry," J. Jortner, R. D. Levine and S. A. Rice Eds. (Interscience Publication, New York, 1981), pp. 713-733.
3. A. Ben-Shaul, Y. Haas, K. L. Kompa and R. D. Levine, "Lasers and chemical change," Springer Series in *Chem. Phys.* **10** (Springer-Verlag, Berlin, 1981).
 4. Aa. S. Subdo, P. A. Schultz, Y. R. Shen and Y. T. Lee, *J. Chem. Phys.* **69**, 2312 (1978); D. J. Krajnovich, A. Giardini-Guidoni, Aa. S. Subdo, P. A. Schultz, Y. R. Shen and Y. T. Lee in "Laser induced processes in molecules," eds. K. L. Kompa and S. D. Smith (Springer-Verlag, Berlin, 1979), pp. 176-178.
 5. D. C. Smith, *J. Appl. Phys.* **41**, 4501 (1970); J. Blazejowski and F. W. Lampe, *Appl. Phys.* **B41**, 109 (1986).
 6. R. N. Haszeldine and K. Leedham, *J. Chem. Soc.* (1952) 3483; C. V. Berney, *Spectrochim. Acta* **21**, 1809 (1965).
 7. P. A. Hackett, C. Willis and M. Gautier, *J. Chem. Phys.* **71**, 2682 (1979).
 8. M. Dronin, P. A. Hackett, C. Willis and M. Gautier, *Can. J. Chem.* **57**, 3053 (1979).
 9. J. Y. Tsao, J. G. Black, E. Yablonovitch and I. Buzak, *J. Chem. Phys.* **73**, 2076 (1980).
 10. A. Gandini and P. A. Hackett, *J. Am. Chem. Soc.* **99**, 6195 (1977).
 11. S. W. Beavan, H. Inone, D. Phyllips and P. A. Hackett, *J. Photochem.* **8**, 247 (1978).
 12. E. Borsella and L. Caneve, *Appl. Phys.* **B46**, 347 (1988).
 13. A. Giardini-Guidoni, A. Mele, R. Teghil, E. Borsella and R. Fantoni, "IR laser photolysis of gaseous polyatomic molecules," Proceedings of S.A.S.P. '88, La Plagne, France, January 1988, p. 389.
 14. W. Batey and A. B. Trenwith, *J. Chem. Soc.* (1961) 1388.
 15. P. A. Hackett and D. Phyllips, *J. Phys. Chem.* **78**, 665 (1974).
 16. P. A. Hackett and D. Phyllips, *J. Phys. Chem.* **78**, 671 (1974).
 17. A. Costela, M. T. Crespo and J. M. Figuera, *J. Photochem.* **34**, 165 (1986); G. D. Greenblatt, S. Ruhman and Y. Haas, *Chem. Phys. Lett.* **112**, 200 (1984).
 18. G. Herzberg, "Molecular spectra and molecular structure—III electronic spectra and electronic structure of polyatomic molecules" (Van Nostrand Reinhold Co., New York, 1966).
 19. K. P. Huber and G. Herzberg, "Molecular spectra and molecular structure—IV constants of diatomic molecules" (Van Nostrand Reinhold Co., New York, 1978).
 20. R. W. B. Pearse and A. G. Gaydon, "The identification of molecular spectra"—III edition (Chapman & Hall Ltd., London, 1965); "Spectroscopic data," vol. 1-2, Eds. S. N. Suchard and J. E. Melzer (IFI/Plenum, New York, 1975).
 21. F. J. de Heer, *Int. J. Radiat. Phys. Chem.* **7**, 137 (1975).
 22. J. H. Kolts and D. W. Setser, "Electronic excited long-lived states of atoms and molecules in flow systems" in "Reactive intermediate in the gas phase" (Academic Press Inc., New York, 1975) pp. 151-222.
 23. A. R. Striganov and N. S. Sventitskii, "Table of spectral lines of neutral and ionized atoms" (IFI/Plenum, New York, 1968); C. E. Moore, "Atomic energy levels," vol. 1, Circular of BNS 467, June 1949; S. Bashkin and J. O. Stiner, Jr., "Atomic energy levels and gortian diagrams 1" (North Holland Publishing Co., Amsterdam, 1975).
 24. I. Kusunoki and Ch. Ottinger, *J. Chem. Phys.* **73**, 2069 (1980).
 25. N. V. Chekalin, V. S. Dolzhikov, V. S. Letokhov, V. N. Likhman and A. N. Shibanov, *Appl. Phys.* **12**, 191 (1977); M. R. Levy, H. Reisler, M. S. Maugir and C. Wittig, *Opt. Engineer.* **19**, 029 (1980); W. Radloff, H. Hohman, H. Albrecht and T. Freudenberg, *Spectrochim. Acta* **43A**, 225 (1987).

26. P. Ho, M. E. Coltrin and W. B. Breiland, "Laser spectroscopy and gas-phase chemistry in C.V.D.," in "Laser processing and diagnostics," D. Bauerle Ed., Springer Series in *Chem. Phys.* **39**, 515 (Springer-Verlag, Berlin, 1984); W. G. Breiland, M. E. Coltrin and P. Ho, *J. Appl. Phys.* **59**, 3267 (1986); W. G. Breiland, P. Ho and M. E. Coltrin, *J. Appl. Phys.* **60**, 1505 (1986).
27. D. A. Cremers, L. J. Radziemski, "Laser plasmas for chemical analysis" in "Laser spectroscopy and its applications." Eds. L. J. Radziemski, R. W. Solaris and J. A. Paisner (M. Dekker Inc., New York, 1987) pp. 351-415.
28. P. J. Hargis, Jr., R. W. Light and J. M. Gee, "Laser diagnostic studies of plasma etching and deposition" in "Laser processing and diagnostics," D. Bauerle Ed., Springer Series in *Chem. Phys.* **39**, 526 (Springer-Verlag, Berlin, 1984).